The EMBO Journal Vol.17 No.12 pp.3309–3316, 1998

Embryonic lethality and abnormal cardiac myocytes in mice lacking ryanodine receptor type 2

Hiroshi Takeshima[1,2,3], Shinji Komazaki[4], Kenzo Hirose[1,2], Miyuki Nishi[1,2], Tetsuo Noda[2,5] and Masamitsu Iino[1,2]

[1]Department of Pharmacology, Faculty of Medicine, University of Tokyo, 7-3-1 Hongo, Bunkyo-ku, Tokyo 113, [2]CREST, Japan Science and Technology Corporation, [4]Department of Anatomy, Saitama Medical School, Moroyama-machi, Saitama 350-01 and [5]Department of Cell Biology, Cancer Institute, Kami-Ikebukuro, Toshima-ku, Tokyo 170, Japan

[3]Corresponding author
e-mail: takeshim@m.u-tokyo.ac.jp

The ryanodine receptor type 2 (RyR-2) functions as a Ca^{2+}-induced Ca^{2+} release (CICR) channel on intracellular Ca^{2+} stores and is distributed in most excitable cells with the exception of skeletal muscle cells. RyR-2 is abundantly expressed in cardiac muscle cells and is thought to mediate Ca^{2+} release triggered by Ca^{2+} influx through the voltage-gated Ca^{2+} channel to constitute the cardiac type of excitation–contraction (E–C) coupling. Here we report on mutant mice lacking RyR-2. The mutant mice died at approximately embryonic day (E) 10 with morphological abnormalities in the heart tube. Prior to embryonic death, large vacuolate sarcoplasmic reticulum (SR) and structurally abnormal mitochondria began to develop in the mutant cardiac myocytes, and the vacuolate SR appeared to contain high concentrations of Ca^{2+}. Fluorometric Ca^{2+} measurements showed that a Ca^{2+} transient evoked by caffeine, an activator of RyRs, was abolished in the mutant cardiac myocytes. However, both mutant and control hearts showed spontaneous rhythmic contractions at E9.5. Moreover, treatment with ryanodine, which locks RyR channels in their open state, did not exert a major effect on spontaneous Ca^{2+} transients in control cardiac myocytes at E9.5–11.5. These results suggest no essential contribution of the RyR-2 to E–C coupling in cardiac myocytes during early embryonic stages. Our results from the mutant mice indicate that the major role of RyR-2 is not in E–C coupling as the CICR channel in embryonic cardiac myocytes but it is absolutely required for cellular Ca^{2+} homeostasis most probably as a major Ca^{2+} leak channel to maintain the developing SR.

Keywords: Ca^{2+} store/caffeine/gene targeting/ryanodine/ryanodine receptor

Introduction

Ca^{2+} signalling is crucial to the regulation of a wide variety of cellular functions, and intracellular Ca^{2+} stores play an essential role in the regulation of the cytoplasmic Ca^{2+} concentration. The ryanodine receptor (RyR) constitutes a major class of intracellular Ca^{2+} release channels in the Ca^{2+} stores (Berridge, 1993) and mediates Ca^{2+}-induced Ca^{2+} release (CICR) which is a mechanism of Ca^{2+} release from the stores, the rate of release being enhanced by increasing cytoplasmic Ca^{2+} concentrations (Endo, 1977; Fabiato and Fabiato, 1978). RyR was first identified as the CICR channel and has been best characterized in skeletal muscle. The purified RyR protein was shown to form a homotetramer with the characteristic 'foot' structure which spans the gap between the membranes of the sarcoplasmic reticulum (SR) and transverse tubule (Fleisher and Inui, 1989; Franzini-Armstrong and Jorgensen, 1994). It was deduced by cloning cDNA that the monomeric RyR is composed of ~5000 amino acid residues with the C-terminal channel region containing transmembrane segments and the remaining large cytoplasmic portion constituting the foot structure (Takeshima *et al.*, 1989). Recent cDNA expression studies identified several functional domains in the primary structure of the RyR molecule. For example, the C-terminal ~20% of the RyR is sufficient to form a functional Ca^{2+} release channel retaining the Ca^{2+}- and ryanodine-binding sites for channel opening but lacking the low-affinity Ca^{2+}-binding site(s) for channel inactivation (Bhat *et al.*, 1997); also the segment of ~100 amino acid residues flanking residue 1350 in the foot region is one of the critical determinants for excitation–contraction (E–C) coupling in skeletal muscle (Yamazawa *et al.*, 1997).

Previous cDNA cloning studies have defined three subtypes of RyR (RyR-1, RyR-2 and RyR-3) that are coded by distinct genes in vertebrates (Meissner, 1994). Briefly, as clarified using subtype-specific probes, RyR-1 is expressed abundantly in skeletal muscle cells, RyR-2 is present predominantly in cardiac muscle cells and at moderate levels in most excitable cells and RyR-3 is expressed at low levels in a wide variety of cell types including most excitable cells and certain non-excitable cells (e.g. Giannini *et al.*, 1995). The knockout mice lacking RyR-1 die perinatally with abnormalities of skeletal muscle, probably due to respiratory failure. In the RyR-1-deficient muscle the contractile response to electrical stimulation under physiological conditions is totally abolished, demonstrating that RyR-1 mediates Ca^{2+} release during E–C coupling in skeletal muscle cells (Takeshima *et al.*, 1994). The knockout mice lacking RyR-3 show apparently normal growth and reproduction with no gross abnormalities. Skeletal muscle from the RyR-3-deficient neonates retained the normal E–C coupling mechanism (Takeshima *et al.*, 1996) but showed reduced contractile responses in comparison with control muscle (Bertocchini *et al.*, 1997). An increased locomotion activity was found in RyR-3-deficient mice, suggesting that Ca^{2+} release via RyR-3 is essential for the function of certain neurons in the central nervous system

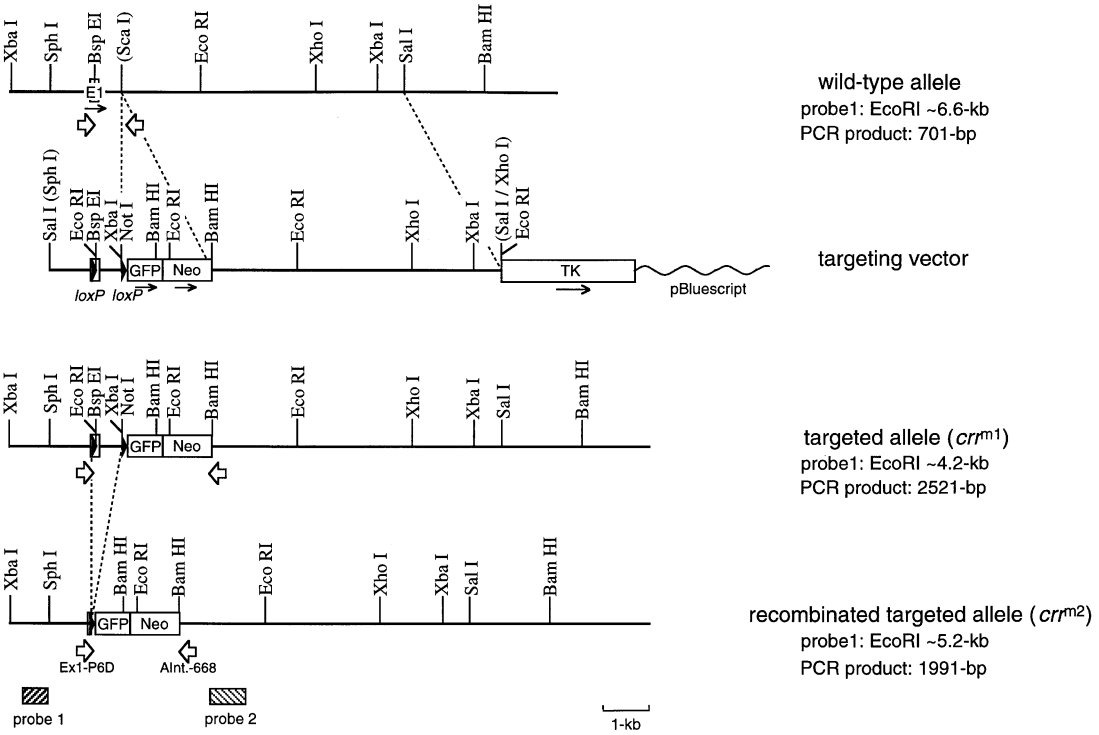

Fig. 1. Mutations introduced into the mouse RyR-2 gene by homologous recombination and Cre-*loxP* recombination. Restriction enzyme maps of the wild-type allele, targeting vector, targeted mutant allele (*crr*^{m1}) and Cre-recombined mutant allele (*crr*^{m2}) are illustrated. The first exon in the gene (E1), GFP, Neo and virus thymidine kinase gene (TK) are indicated by open boxes; the directions of transcription are indicated by arrows. In the targeting vector, the *loxP* sequence was introduced into the *Bsp*EI site of the 5′-untranslated region in exon 1, and the *loxP*–GFP–Neo cassette was inserted into the *Sca*I site in intron 1. The genomic DNA probes and PCR primers for detection of the mutations are indicated by hatched boxes and opened arrows, respectively; predicted sizes of DNA fragments in the Southern blot analysis and the PCR are also shown. The nucleotide sequence of the exon 1 and intron 1 in the gene was submitted to the DDBJ/EMBL/GenBank database with the accession No. AB012003.

(Takeshima *et al.*, 1996). The double-knockout mice lacking both RyR-1 and RyR-3 exhibit defective skeletal muscle cells with no CICR activities and severe morphological abnormalities (Ikemoto *et al.*, 1997). On the other hand, knockout mice lacking RyR-2 have not yet been reported, and the generation and examination of such mutant mice may be important in determining the physiological roles of Ca^{2+} signalling via RyR-2.

The functions of RyR-2, which is thought to constitute the CICR channel with the highest Ca^{2+} sensitivity among RyR subtypes, have been well-characterized in the heart. In mature cardiac muscle cells, Ca^{2+} influx through the voltage-dependent L-type Ca^{2+} channel is thought to trigger the activation of Ca^{2+} release via RyR-2 by the CICR mechanism, and the amplified Ca^{2+} signalling causes muscle contraction (Fabiato, 1985; Nabauer *et al.*, 1989). In contrast to the essential role of RyR-2 in mature cardiac myocytes, previous studies have suggested that the Ca^{2+} available for E–C coupling in the fetal heart is derived from Ca^{2+} influx through the voltage-dependent Ca^{2+} channel (Fabiato and Fabiato, 1978; Klitzner and Friedman, 1989), and therefore the function of RyR-2 during myocardial development is not yet clear. In this report, we describe a novel physiological role of RyR-2 in the fetal heart on the basis of results from morphological and physiological analyses of knockout mice lacking RyR-2.

Results and discussion

Generation of mutant mice lacking RyR-2

A genomic DNA clone carrying the first exon of the mouse RyR-2 gene was isolated, and the DNA insert was used to construct a targeting vector (Figure 1). In the vector, the *loxP* sequence for the Cre recombinase-mediated DNA recombination (Sauer and Henderson, 1988) was introduced into the 5′-untranslated region, and another *loxP* sequence, linked to the green fluorescence protein-coding sequence (GFP) and the neomycin resistance gene without the polyadenylation signal (Neo), was inserted into the first intronic sequence of the gene. J1 embryonic stem (ES) cells were transfected with the targeting vector, and ES clones containing the homologously recombined gene, designated *crr*^{m1}, were isolated. The ES cells carrying the *crr*^{m1}allele were further treated with adenovirus vectors for transient expression of Cre recombinase to establish ES clones carrying the recombined mutant gene referred to as *crr*^{m2}. In the *crr*^{m2} allele the first protein-coding sequence of 48 base pairs and the partial sequence of the first intron are deleted from the RyR-2 gene. The ES clones harbouring the introduced mutant genes showed the expected pattern of arrangement in genomic DNA by Southern blot hybridization analysis using several restriction enzymes and specific probes for the gene (Figure 2A; Materials and methods).

Chimeric male mice were generated using the ES cells

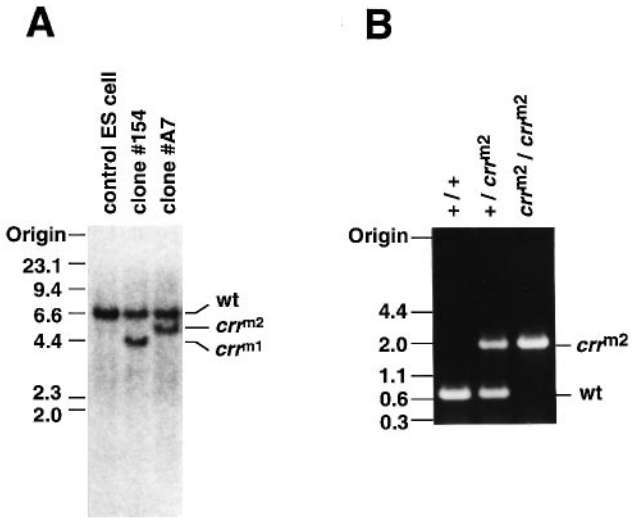

Fig. 2. Detection of mutant RyR-2 genes. (**A**) Southern blot analysis of DNAs from ES clones containing mutant RyR-2 genes. DNAs from ES cells were digested with *Eco*RI and analysed. The hybridization probe (probe 1) used and the expected sizes of the positive restriction fragments are shown in Figure 1. ES clones #154 and #A7 contain the *crr*^{m1} and *crr*^{m2} mutant genes, respectively. (**B**) Detection of the *crr*^{m2} mutant gene by PCR using genomic DNAs from mouse embryos. Primers used for amplification and the expected sizes of the products are shown in Figure 1. The size markers are indicated in kilobase pairs.

thus isolated, and bred to yield mice carrying the mutant genes. The *crr*^{m1} mutation is thought to be a silent mutation in the RyR-2 gene, because the mutant mice homozygous for *crr*^{m1} exhibited no abnormalities in growth, health or reproduction over a 1 year period (H.Takeshima and M.Nishi, unpublished observation). On the other hand, we could not generate neonates homozygous for *crr*^{m2}. However, the embryos homozygous for *crr*^{m2}, identified by the polymerase chain reaction (PCR) (Figure 2B), were found in the early developmental stages. At embryonic day (E) 8.5 and E9.5 the homozygous mutant mice were alive, but all of the mutants obtained were dead at E10.5 or E11.5 (Table I). This, together with the results of physiological experiments described below, indicates that the mutation of *crr*^{m2} is a null mutation in the mouse RyR-2 gene associating an embryonic lethality at around E10.5 in the homozygous state. The characteristic features of the RyR-2-deficient mutant mice with the *crr*^{m2}/*crr*^{m2} genotype are described in the following sections of this report. In the morphological and physiological experiments no significant differences were observed between wild-type and +/*crr*^{m2} mice.

Histological abnormalities in mice lacking RyR-2

The RyR-2-deficient embryos showed no significant morphological abnormalities at E8.5 but the mutants exhibited slightly delayed development in size and appearance compared with control embryos at E9.5 (Figure 3). In both mutant and control E8.5 embryos, the looped heart tubes were formed but no spontaneous contractions were detected. At E9.5 spontaneous rhythmic contractions of the heart were observed in embryos of both genotypes (see section below). However, the E10.5 mutant embryos exhibited no heart beats and congestive peripheral tissues, and their anatomical features were similar to those of E9.5

Table I. Genotype of pups obtained by crosses between +/*crr*^{m2} mice

	crr^{m2}/*crr*^{m2}	+/*crr*^{m2}	+/+
E8.5	3	12	8
E9.5	24	38	32
E10.5	18[a]	31	30
E11.5	12[b]	15	9
E12.5	1[b]	3	3
neonates	0	32	22

[a]Embryos exhibiting cardiac arrest and congestive perpheral tissues.
[b]Embryos exhibiting autolysis.

embryos. At E11.5 the mutant embryos were white in colour and their bodies showed autolysis. Thus, the embryonic development of the RyR-2-deficient mice is inhibited during E8.5–9.5 and is interrupted at E9.5.

Significant histological abnormalities in the mutant embryos at E9.5 were found in the heart (Figure 3). In control E9.5 hearts, the myocardium and trabeculae composed of one to three myocyte layers were developing well and the epicardium, the single cell layer surrounding the heart, was organized. In the mutant hearts on the other hand, the myocardium and trabeculae were arranged irregularly and the epicardium was not well-organized. The results indicate that RyR-2 deficiency interferes with the maturation and development of the heart.

The histological abnormalities of the heart may or may not be the cause of lethality of the mutant mice in the early developmental stages, because RyR-2 is expressed in most excitable cells except for skeletal muscle cells in adult mice and may participate in as yet unknown essential functions. However, in the E9.5 mutant embryos, we could not detect clear histological abnormalities in the developing neural tubule, blood vessels or primitive digestive organs, that contain immature neurons or smooth muscle cells. It is therefore likely that RyR-2 deficiency primarily damages embryonic cardiac myocytes.

Ultrastructural abnormalities in cardiac myocytes from mice lacking RyR-2

We examined the ultrastructure of cardiac myocytes from the RyR-2-deficient embryos (Figure 4). The rough endoplasmic reticulum (rER) was partly swollen at E8.5 and many vacuoles were generated at E9.5 and E10.5 in the mutant cardiac myocytes. The vacuoles were developing in size during the embryonic stages; the diameters of the swollen rER or the vacuoles were <0.2 μm at E8.5, 0.2–0.8 μm at E9.5 and 2–5 μm at E10.5. No such swollen rER or vacuoles were detected in control myocytes. These observations, together with the fact that the SR is derived from rER (Flucher, 1992), indicate that the abnormal vacuoles observed in the mutant myocytes correspond to developing SR vesicles. This conclusion is supported by the observation that the rER disappeared in the E9.5 and E10.5 mutant myocytes. Moreover, most mitchondria exhibited tubular cristae and were structurally abnormal in the mutant myocytes; they were smaller than those in controls at E9.5 and exhibited swollen and round structures at E10.5. The abnormalities of the cytoplasmic organelles could not be found in other tissues examined in the mutant embryos, including epiderm, mesenchyme and neural tube. The ultrastructural abnormalities in the RyR-2-deficient

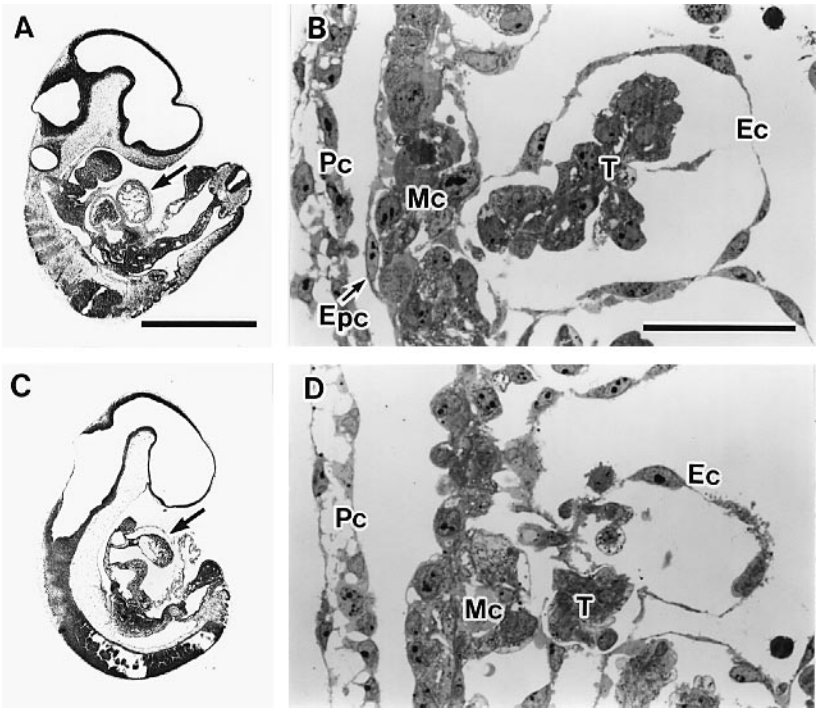

Fig. 3. Features and histological abnormalities in heart of E9.5 RyR-2-deficient mice. In comparison with wild-type littermates (**A**), a slight delay in developmental progress was observed in the E9.5 mutant embryos (**C**), for example, in the compartmentalization of the central nervous system and in the turning process of somites. Arrow shows the looped cardiac tubule of the embryonic heart. The features of the E9.5 mutant embryos are likely to correspond to those of about E9.0 controls, but the mutants showed no gross abnormalities in the organization of tissues. In the ventricular wall of the wild-type heart from E9.5 embryos (**B**), the myocardium and trabeculae were well-developed, and the epicardium was organized. In the mutant heart (**D**), abnormal arrangements of myocytes constituting the myocardium and trabeculae were observed, and the epicardium was not organized. Pc, pericardium; Epc, epicardium; Mc, myocardium; T, trabeculae; Ec, endocardium. Scale bars: 1 mm in (A) and (C); 50 μm in (B) and (D). Representative data are shown from the observation of wild-type ($n = 5$), $+/crr^{m2}$ ($n = 7$) and crr^{m2}/crr^{m2} ($n = 8$) embryos.

cardiac myocytes might cause the histological derangement of the heart described in the above section.

To examine the localization of Ca^{2+}, cardiac myocytes were treated with fixatives containing oxalate and ferricyanide and analysed under an electron microscope equipped with an X-ray microanalyser (Figure 5). In E9.5 mutant myocytes the abnormal vacuoles contained electron-dense deposits that were identified as precipitates of calcium oxalate by the X-ray microanalysis. The vacuoles therefore contained enough Ca^{2+} to form precipitates with oxalate. However, in control experiments using wild-type myocytes we did not detect such electron-dense deposits in intracellular organelles (data not shown). The results suggest that Ca^{2+} overloading results in the generation of abnormal vacuoles from the developing SR in mutant cardiac myocytes.

RyRs can be identified as foot structures by electron microscopic observation clustered in junctional gaps between the cell surface and intracellular vesicular membranes (Franzini-Armstrong and Jorgensen, 1994). However, in cardiac myocytes from E9.5 or E10.5 control embryos we could not observe either clustered foot structures or junctional structures between the SR and cell-surface membranes. The results in the embryonic myocytes indicate not only the low content of RyR-2 but also the absence of co-localization of the L-type Ca^{2+} channel and the RyR-2. The co-localization of the channel proteins is thought to be required for E–C coupling of mature cardiac muscle cells (Sun *et al.*, 1995).

Surplus cells are removed by apoptotic cell death during embryonic development, and apoptosis is known to accompany morphological changes including cell shrinkage and condensation of nuclei (Jacobson and Raff, 1997). However, mutant cardiac myocytes from the E9.5 or E10.5 embryos did not show such characteristic features of apoptosis (data not shown). It is probable that the mode of cell death in the mutant cardiac myocytes is necrosis.

Ca^{2+} signalling in cardiac myocytes from mice lacking RyR-2

We investigated Ca^{2+} signalling in embryonic myocytes using Fluo-3 as a Ca^{2+} indicator. Cardiac myocytes from both mutant and control embryos at E9.5 showed spontaneous Ca^{2+} oscillations (Figure 6). This is consistent with the presence of rhythmic contractions of hearts in both genotypes. The control myocytes showed Ca^{2+} transients upon application of caffeine, an activator of RyR subtypes, in a Ca^{2+}-free bathing solution. In contrast, no response to caffeine was detected in the mutant myocytes. These results indicate that the mutant cardiac myocytes do not express any known RyR subtypes which are sensitive to caffeine and also suggest that RyR-2 exists in control myocytes at E9.5.

To determine the possible contribution of RyR-2 to E–C coupling in the embryonic hearts, cardiac myocytes from E10.5 wild-type embryos were treated with ryanodine, which binds to activated RyRs to lock them in the open state and hence irreversibly depletes the intracellular Ca^{2+} stores. The increase in intracellular Ca^{2+} concentration during spontaneous contractions was still retained

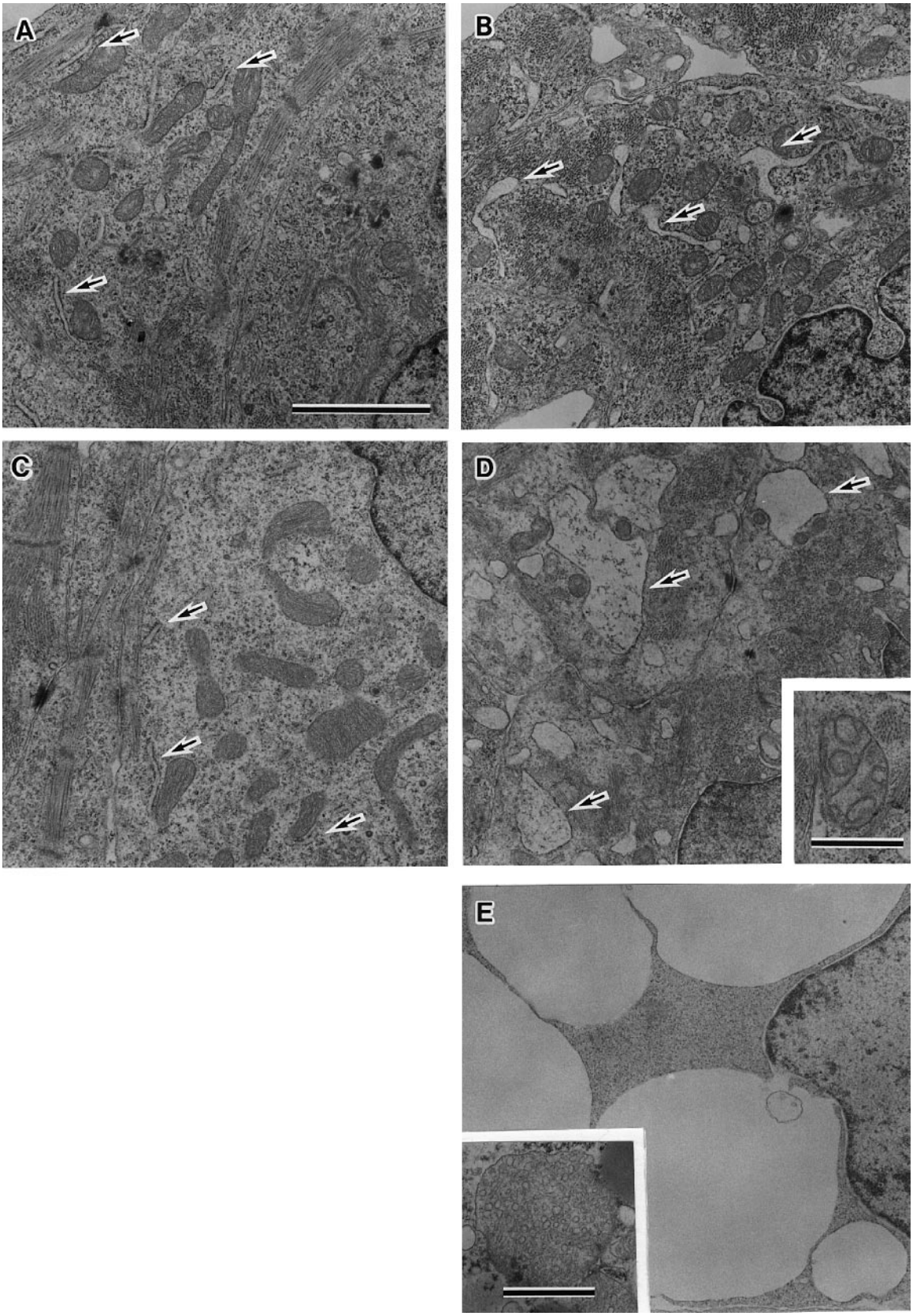

Fig. 4. Ultrastructural abnormalities in cardiac myocytes from E8.5–10.5 RyR-2-deficient embryos. Electron micrographs were obtained from cardiac myocytes in (**A**) E8.5 wild-type, (**B**) E8.5 mutant, (**C**) E9.5 wild-type, (**D**) E9.5 mutant and (**E**) E10.5 mutant embryos. Abnormally large vacuoles were found in mutant myocytes, and the growth of the vacuoles in size were observed during the embryonic development in the mutant mice. The normal rER (or developing SR) in control myocytes and the rER carrying swelling parts and abnormal vacuoles in mutant myocytes are indicated by arrows. The majority of mitochondria with abnormal tubular cristae were smaller at E9.5 and swelling at E10.5 in the mutant myocytes (insets in D and E). Scale bars: 5 μm in (A)–(E); 1 μm in insets of (D) and (E). Representative data are shown from the observation of wild-type (E8.5, $n = 3$; E9.5, $n = 5$; E10.5, $n = 6$), $+/crr^{m2}$ (E8.5, $n = 3$; E9.5, $n = 7$; E10.5, $n = 6$) and crr^{m2}/crr^{m2} (E8.5, $n = 3$; E9.5, $n = 8$; E10.5, $n = 6$) embryos.

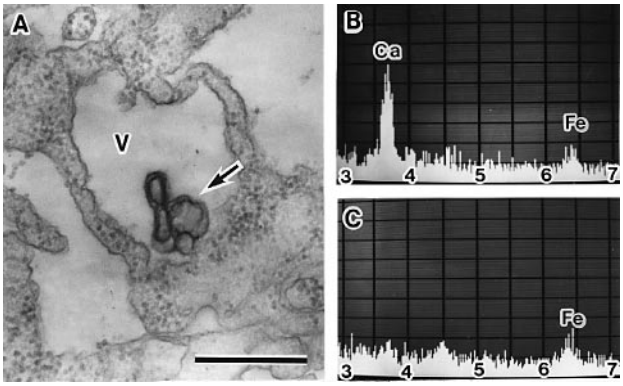

Fig. 5. High Ca^{2+} contents in abnormal vacuoles in E9.5 mutant cardiac myocytes lacking RyR-2. The mutant myocytes were treated with oxalate and the resulting precipitates of calcium oxalate were visualized with ferricyanide as electron-dense materials (arrow) on electron-microscopic observation (**A**). Scale bar, 0.5 μm. X-ray spectra were obtained from the electron-dense deposit (**B**) and cytoplasm devoid of vacuole (**C**). Vertical scales indicate 100 counts/division, and numbers on the horizontal scales indicate KeV. In control experiments using E9.5 wild-type hearts, such electron-dense deposits were not observed in intracellular organelles. Representative data are shown from observations of wild-type ($n = 2$) and crr^{m2}/crr^{m2} ($n = 2$) embryos.

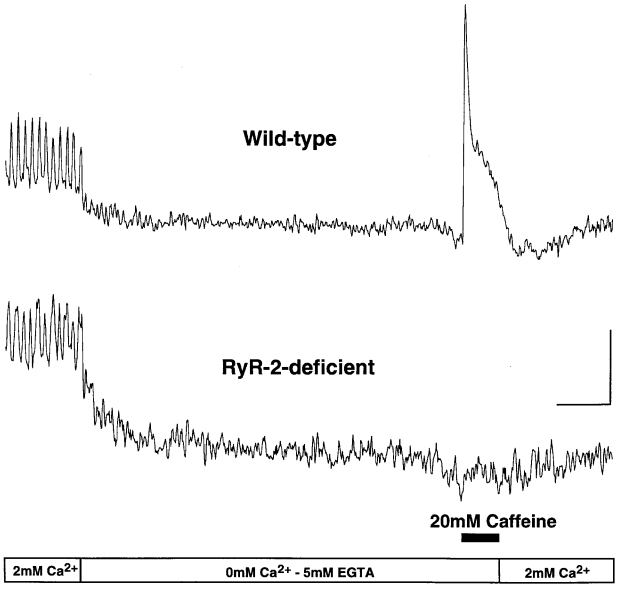

Fig. 6. Spontaneous Ca^{2+} oscillations and loss of caffeine-evoked Ca^{2+} transients in cardiac myocytes from E9.5 RyR-2-deficient embryos. Intracellular Ca^{2+} concentrations of myocytes from wild-type (upper trace) and RyR-2-deficient (lower trace) embryos were measured with Fluo-3, and the time course of change in fluorescence intensity is shown. Ca^{2+} oscillations in both cell types were abolished in a Ca^{2+}-free solution containing 5 mM EGTA. The application of 20 mM caffeine in the Ca^{2+}-free bathing solution induced Ca^{2+} transients in control cells, but not in the mutant cells. The horizontal scale indicates 20 s, and the vertical scale indicates 10% change in fluorescence intensity in upper trace and 5% in lower trace, relative to the diastolic level. Representative data are shown from the experiments in wild-type ($n = 9$), $+/crr^{m2}$ ($n = 15$) and crr^{m2}/crr^{m2} ($n = 7$) embryos.

after ryanodine treatment, even though depletion of the stores was confirmed by the absence of response to subsequent application of caffeine (Figure 7). Similar results were obtained in control myocytes from E9.5 and E11.5 embryos. These data therefore suggest that the loss

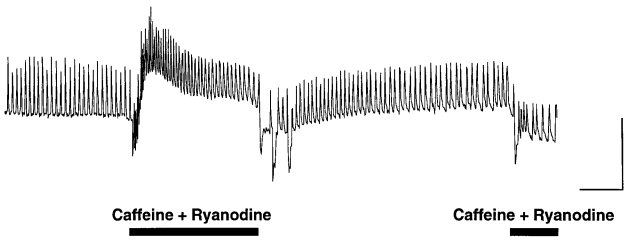

Fig. 7. Effect of ryanodine on spontaneous Ca^{2+} oscillations in E10.5 cardiac myocytes from wild-type embryos. The time course of change in fluorescence intensity of Fluo-3 is shown. Ryanodine (100 μM) was applied with caffeine (20 mM), because the binding of ryanodine to RyR is enhanced when the RyR channel is activated by caffeine. Depletion of the Ca^{2+} stores was confirmed by the second amplification of caffeine and ryanodine. Essentially the same results were obtained for E9.5 and E11.5 control myocytes. The horizontal scale indicates 20 s, and the vertical scale represents 10% change in fluorescence intensity relative to the diastolic level. Downward deflections were due to movement of the specimen by solution exchange. Representative responses are shown from the experiments in wild-type (E9.5, $n = 11$; E10.5, $n = 8$; E11.5, $n = 2$) and $+/crr^{m2}$ (E9.5, $n = 15$; E10.5, $n = 9$; E11.5, $n = 8$) embryos.

of the CICR via RyR-2 does not abolish E–C coupling in the early embryonic stages. In accordance with this notion, previous studies in rat have suggested that Ca^{2+} for E–C coupling in fetal heart is derived mainly from Ca^{2+} influx through the voltage-gated Ca^{2+} channels (Fabiato and Fabiato, 1978; Klitzner and Friedman, 1989).

Role of RyR-2 in developing fetal heart

We have reported previously that RyR-2 expressed in cultured skeletal muscle cells evokes depolarization-independent spontaneous Ca^{2+} sparks and waves (Yamazawa *et al.*, 1996). This observation is thought to reflect the opening of the RyR-2 channel at resting intracellular Ca^{2+} levels and that RyR-2 has the highest Ca^{2+} sensitivity among the RyR subtypes. The RyR-2 channel may open occasionally, even at resting intracellular Ca^{2+} levels, in fetal cardiac myocytes, although Ca^{2+} release does not primarily contribute to E–C coupling. On the other hand, mutant cardiac myocytes losing functional CICR channel activity contain the large vacuoles of the SR and abnormal mitochondria. The ultrastructural defects of the cytoplasmic organelles are essentially the same as those found in skeletal muscle cells from double-mutant mice lacking both RyR-1 and RyR-3 (Ikemoto *et al.*, 1997). Skeletal muscle cells contain RyR-1 and RyR-3 as the predominant and minor components of the Ca^{2+} release channels, respectively, but the mutant myocytes lacking either RyR-1 or RyR-3 do not exhibit such severe ultrastructural defects as in the double-mutants (Takeshima *et al.*, 1994, 1996). Based on two independent examples, the mutant cardiac myocytes lacking RyR-2 and the double-mutant skeletal muscle cells lacking both RyR-1 and RyR-3, it seems reasonable to conclude that both abnormalities of the organelles are caused by the complete loss of the Ca^{2+} release channel as a safety valve for intracellular Ca^{2+} stores. Without the Ca^{2+} release channel, Ca^{2+} stores may become overloaded with cytoplasmic Ca^{2+}. Such Ca^{2+} overloading is thought to be more severe in mutant cardiac myocytes than in double-mutant skeletal muscle cells, because continuous Ca^{2+} oscillations accompany greater Ca^{2+} influxes through cardiac L-type Ca^{2+} channels,

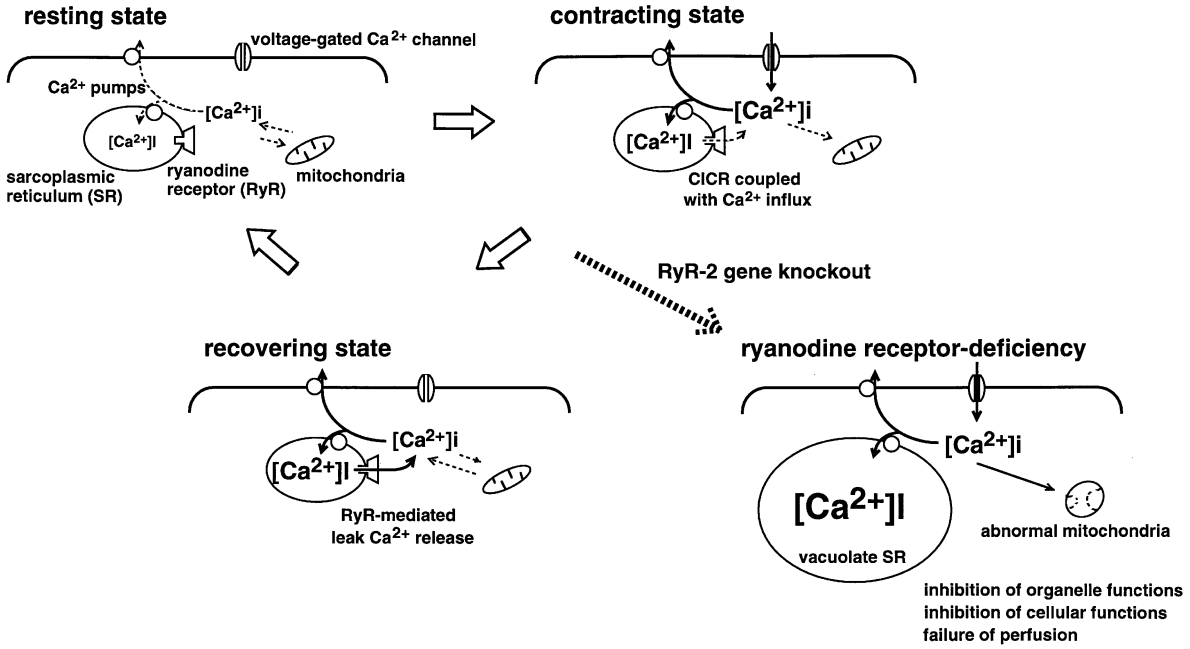

Fig. 8. Proposed role of RyR-2 on developing Ca^{2+} stores in embryonic cardiac myocytes. Major intracellular Ca^{2+} flow is represented schematically. Even though only a slight contribution to the Ca^{2+} signalling during E–C coupling can be detected, RyR-2 probably functions as a safety valve in developing Ca^{2+} stores for the release of overloaded luminal Ca^{2+}. Without RyR-2, the overloading of Ca^{2+} may induce vacuole formation of the developing SR, then the disfunction of the SR may cause mitochondrial abnormalities and finally myocytes may not contribute to the body-fluid circulation.

which have a higher conductance than skeletal muscle counterparts.

On the basis of the above observations, we propose that RyR-2 does not participate principally in Ca^{2+} signalling during E–C coupling in the embryonic heart but functions as a major leak Ca^{2+} channel to maintain the normal range of luminal Ca^{2+} levels in the developing SR. In cardiac myocytes lacking RyR-2, cytoplasmic Ca^{2+} derived from extracellular fluid during E–C coupling may be gradually accumulated in the SR lacking RyR-2 as a leak Ca^{2+} channel, then cytoplasmic Ca^{2+} which cannot be sequestered by the overloaded SR may flow into mitochondria, and finally defective organelles and/or abnormal Ca^{2+} homeostasis may cause dysfunction of mutant cardiac myocytes (Figure 8). Thus, our present study indicates a novel physiological role for the RyRs in developing intracellular Ca^{2+} stores. Local intracellular Ca^{2+} transients caused by the activation of several RyR channels on the SR can be detected as Ca^{2+} sparks in cardiac muscle cells and Ca^{2+} sparks are proposed to be the unitary events underlying cardiac E–C coupling (Cannell *et al.*, 1995; Lopez-Lopez *et al.*, 1995). In addition, Ca^{2+} sparks might reflect RyR-mediated leak Ca^{2+} release for the maintenance of Ca^{2+} concentration in stores. It is an attractive hypothesis that in order to prevent store overloading, RyR channels may be activated in response to elevation of luminal Ca^{2+} levels. This idea may be supported by previous bilayer studies which indicate the luminal Ca^{2+} dependency of RyR activation (Sitsapesan and Williams, 1997).

Materials and methods

Generation of mutant mice

The rabbit RyR-2 cDNA fragment (nucleotide residues –54 to 49; Nakai *et al.*, 1990) was amplified by PCR using synthetic primers. A mouse genomic DNA library was screened with the amplified fragment as a probe to yield λMHRRG153 carrying the 5′-terminal region of the RyR-2 gene. The targeting vector was constructed using the genomic DNA fragments obtained, synthetic linkers carrying the *loxP* sequence (Shibata *et al.*, 1997), the GFP-coding region from pGreen Lantern-1 (Gibco-BRL), the neomycin-resistance gene from pMC1 Neo (Stratagene), the virus thymidine kinase gene (Takeshima *et al.*, 1994) and pBluescript SK(–) (Stratagene). The short arm of the vector is the 1.0 kb *Sph*I–*Bsp*EI fragment containing the putative promoter and 5′-untranslated sequences, and the long arm is the 6.5 kb fragment containing the first intronic sequence (Figure 1).

J1 ES cells (Li *et al.*, 1992) were transfected with the linearized targeting vector and selected using G418 and FIAU (Takeshima *et al.*, 1994). Of ~300 clones isolated, Southern blotting analysis identified four clones carrying the homologous mutation (*crr*^{m1}) including the ES clone numbered 154. The #154 cells were inoculated with the recombinant adenovirus (AxSRαCre) for transient expression of Cre recombinase (Shibata *et al.*, 1997) and several clones, including the clone numbered A7, were selected as the ES cells containing the recombined mutant gene (*crr*^{m2}). The mutations introduced into the clones were further confirmed by Southern blot analysis using several restriction enzymes (*Eco*RI, *Xba*I, *Bam*HI and *Xho*I) and two different probes from the 5′-flanking region (probe 1) and first intron (probe 2) as shown in Figure 1. The production of chimeric mice using ES clones and mutant mice homozygous for *crr*^{m1} or *crr*^{m2} was carried out essentially as described previously (Takeshima *et al.*, 1994). To determine the genotypes of the mutant mice, PCR was carried out using primers from the genomic sequence, the forward primer (Ex1-P6D, 25mer: GAGCCCCTA-GAACATCCTGGTTAGC) and the reverse primer (AInt-668, 25mer: GCTGAGAAGGCTGCCCCCAGGGTGC). The expected sizes of amplified DNA fragments from the wild-type, *crr*^{m1} and *crr*^{m2} alleles are shown in Figure 1.

Anatomical analyses

Mouse embryos were treated with a pre-fixative buffer containing 3% paraformaldehyde, 2.5% glutaraldehyde and 0.1 M sodium cacodylate, pH 7.5. After washing with the buffer solution, they were fixed with a post-fixative solution containing 1% OsO_4, 0.1 M sodium cacodylate, pH 7.5, and then the fixed embryos were dehydrated and embedded in Epon. For light-microscopy observation, 0.5 μm sections were prepared and stained with 0.1% toluidine blue solution. For ultrastructural analysis

using an electron microscope (JEOL, JEM-200CX), 80–90 nm sections were prepared and stained with uranyl acetate and lead citrate.

In an attempt to determine the ultrastructural localization of Ca^{2+}, fetal hearts were treated with the pre-fixative buffer supplemented with 50 mM potassium oxalate and then post-fixed in a solution containing 1% OsO_4, 0.1 M potassium ferricyanide and 0.1 M sodium cacodylate, pH 7.5. After dehydration, the tissues were embedded in Epon, and 100–150 nm sections were prepared and observed without staining. The X-ray microanalysis was performed on sections using a Delta Level-IV X-ray analyser (Kevex Co., Foster City, USA) as described previously (McGrew *et al.*, 1980; Komazaki and Hiruma, 1994).

Ca^{2+} measurements

Mouse embryonic hearts were isolated and fixed on silicone rubber with stainless steel pins. The tissue was submerged in a physiological salt solution (PSS; 150 mM NaCl, 4 mM KCl, 2 mM $CaCl_2$, 1 mM $MgCl_2$, 5 mM HEPES, 5.6 mM glucose, pH 7.4) containing 5 μM Fluo-3 AM and 0.1% bovine serum albumin for ~1 h. The heart mounted on silicone rubber was placed on a glass-bottomed culture dish (MatTak Corp., USA). A cooled CCD camera (Photometrics) mounted on the microscope (IX-70, Olympus), equipped with a polychromatic illumination system (TILL Photonics, Germany), was used to capture the fluorescence images with excitation at 470 nm and emission at >510 nm at 4 frames/s. The experiments were carried out at room temperature.

Acknowledgements

We thank Akiko Sakamoto, Izumi Dobashi and Hitomi Yamanaka for their help with some of the experiments and for maintaining the mutant mice. This work was supported in part by grants from the Ministry of Education, Science, Culture and Sports, the Life Science Foundation and TMFC.

References

Berridge,M.J. (1993) Inositol trisphosphate and calcium signalling. *Nature*, **361**, 315–325.

Bertocchini,F., Ovitt,C.E., Conti,A., Barone,V., Scholer,H.R., Bottinelli,R., Reggiani,C. and Sorrentino,V. (1997) Requirement for the ryanodine receptor type 3 for efficient contraction in neonatal skeletal muscles. *EMBO J.*, **16**, 6956–6963.

Bhat,M.B., Zhao,J., Takeshima,H. and Ma,J. (1997) Functional calcium release channel formed by the carboxyl-terminal portion of ryanodine receptor. *Biophys. J.*, **73**, 1329–1336.

Cannell,M.B., Cheng,H. and Lederer,W.J. (1995) The control of calcium release in heart muscle. *Science*, **268**, 1045–1049.

Endo,M. (1977) Calcium release from the sarcoplasmic reticulum. *Physiol. Rev.*, **57**, 71–108.

Fabiato,A. (1985) Simulated calcium current can both cause calcium loading in and trigger calcium release from the sarcoplasmic reticulum of a skinned canine cardiac Purkinje cell. *J. Gen. Physiol.*, **85**, 291–320.

Fabiato,A. and Fabiato,F. (1978) Calcium triggered release of calcium from the sarcoplasmic reticulum of skinned cells of adult human, dog, cat, rabbit, rat and frog heart and fetal and newborn rat ventricules. *Ann. N. Y. Acad. Sci.*, **307**, 491–522.

Fleisher,S. and Inui,M. (1989) Biochemistry and biophysics of excitation–contraction coupling. *Annu. Rev. Biophys. Biophys. Chem.*, **18**, 333–364.

Flucher,B.E. (1992) Structural analysis of muscle development; transverse tubules, sarcoplasmic reticulum, and the triad. *Dev. Biol.*, **154**, 245–260.

Franzini-Armstrong,C. and Jorgensen,A.O. (1994) Structure and development of E–C coupling units in skeletal muscle. *Annu. Rev. Physiol.*, **56**, 509–534.

Giannini,G., Conti,A., Mammarella,S., Scrogna,M. and Sorrentino,V. (1995) The ryanodine receptor/calcium release channel genes are widely and differentially expressed in murine brain and peripheral tissues. *J. Cell Biol.*, **128**, 893–904.

Ikemoto,T., Komazaki,S., Takeshima,H., Nishi,M., Noda,T., Iino,M. and Endo,M. (1997) Functional and morphological features of skeletal muscle from mutant mice lacking both type 1 and type 3 ryanodine receptors. *J. Physiol.*, **501**, 305–312.

Jacobson,M.D. and Raff,M.C. (1997) Programmed cell death in animal development. *Cell*, **88**, 347–354.

Klitzner,T.M. and Friedman,W.F. (1989) A diminished role for the sarcoplasmic reticulum in newborn myocardial contraction: effects of ryanodine. *Pediatr. Res.*, **26**, 98–101.

Komazaki,S. and Hiruma,T. (1994) Calcium-containing vacuolated mitochondria during early heart development in chick embryos as demonstrated by cytochemistry and X-ray microanalysis. *Anat. Embryol.*, **189**, 441–446.

Li,E., Bestor,T.H. and Jaenisch,R. (1992) Targeted mutation of the DNA methyltransferase gene results in embryonic lethality. *Cell*, **69**, 915–926.

Lopez-Lopez,J.R., Shacklock,P.S., Balke,C.W. and Wier,W.G. (1995) Local calcium transients triggered by single L-type calcium channel currents in cardiac cells. *Science*, **268**, 1042–1045.

McGrew,C.F., Somlyo,A.V. and Blaustein,M.P. (1980) Localization of calcium in presynaptic nerve terminals. An ultrastructural and electron microscope analysis. *J. Cell Biol.*, **85**, 228–241.

Meissner,G. (1994) Ryanodine receptor/Ca^{2+} release channels and their regulation of endogenous effectors. *Annu. Rev. Physiol.*, **56**, 485–508.

Nabauer,M., Callewaert,G., Cleenman,L. and Morad,M. (1989) Regulation of calcium release is gated by calcium current not gating charge in cardiac myocytes. *Science*, **244**, 800–803.

Nakai,J., Imagawa,T., Hakamata,Y., Shigekawa,M., Takeshima,H. and Numa,S. (1990) Primary structure and functional expression from cDNA of the cardiac ryanodine receptor/calcium release channel. *FEBS Lett.*, **271**, 169–177.

Sauer,B. and Henderson,N. (1988) Site-specific DNA recombination in mammalian cells by the Cre recombinase of bacteriophage P1. *Proc. Natl Acad. Sci. USA*, **85**, 5166–5170.

Shibata,H. *et al.* (1997) Rapid colorectal adenoma formation initiated by conditional targeting of the Apc gene. *Science*, **278**, 120–123.

Sitsapesan,R. and Williams,A.J. (1997) Regulation of current flow throgh ryanodine receptors by luminal Ca^{2+}. *J. Membr. Biol.*, **159**, 179–185.

Sun,X.-H., Protasi,F., Takahashi,M., Takeshima,H., Ferguson,D.G. and Franzini-Armstrong,C. (1995) Molecular architecture of membranes involved in excitation–contraction coupling of cardiac muscle. *J. Cell Biol.*, **129**, 659–671.

Takeshima,H. *et al.* (1989) Primary structure and expression from complementary DNA of skeletal muscle ryanodine receptor. *Nature*, **339**, 439–445.

Takeshima,H., Iino,M., Takekura,H., Nishi,M., Kuno,J., Minowa,O., Takano,H. and Noda,T. (1994) Excitation–contraction uncoupling and muscular degeneration in mice lacking functional skeletal muscle ryanodine-receptor gene. *Nature*, **369**, 556–559.

Takeshima,H. *et al.* (1996) Generation and characterization of mutant mice lacking ryanodine receptor type 3. *J. Biol. Chem.*, **271**, 19649–19652.

Yamazawa,T., Takeshima,H., Sakurai,T., Endo,M. and Iino,M. (1996) Subtype specificity of the ryanodine receptor for Ca^{2+} signal amplification in excitation–contraction coupling. *EMBO J.*, **15**, 6172–6177.

Yamazawa,T., Takeshima,H., Shimuta,M. and Iino,M. (1997) A region of the ryanodine receptor critical for excitation–contraction coupling in skeletal muscle. *J. Biol. Chem.*, **272**, 8161–8164.

Received March 5, 1998; revised April 15, 1998; accepted April 16, 1998